

PERFORMANCE ANALYSIS OF A 3D SCRAMJET INTAKE

Birgit U. Reinartz
CATS, RWTH Aachen University, Germany

Keywords: *scramjet, hypersonic, intake, CFD*

Abstract

A combined experimental as well as computational analysis of a complete scramjet demonstrator model has been initiated. The experimental tests will take place under real flight conditions at a hypersonic wind tunnel. Prior to those tests, a numerical analysis of the performance of the demonstrator geometry is conducted. In the current paper, the results of the performance analysis for the newly designed three-dimensional intake employing a single outer compression ramp as well as side wall compression are discussed. It is shown that the intake is able to generate flow conditions required for stable supersonic combustion using a central strut injector.

1 Introduction

Within the frame of the Research Training Group (GRK) "Aerothermodynamic Design of a Scramjet Engine for Future Space Transportation Systems", a combined numerical as well as experimental analysis of a complete scramjet demonstrator model has been initiated. The experimental tests are being performed under real flight conditions at the hypersonic wind tunnel AT-303 of the Institute of Theoretical and Applied Mechanics (ITAM) in Novosibirsk, Russia. One of the key interests of the Research Training Group is proving that central strut injectors perform best for large combustors as they are needed for civil applications in space transportation. Two different central strut injectors which have been developed in Germany over the last decade [7] will be tested during the test campaign in Russia. So far these injectors have only been used in connected

pipe facilities where the flow obstruction due to the struts had a large effect on the performance. The pending demonstrator tests are a much appreciated opportunity to test those injectors under improved conditions because a larger combustion chamber will be realized. Before, a variation of a 3D mixed compression inlet tested before at ITAM [6] was analyzed for the pending tests. However, the analyzes showed the height of the intake exit to be too small to obtain good strut injector conditions [13]. Thus, a new 3D intake was designed (see Fig. 1) using a single compression ramp with a deflection of 14 degrees and a sweep angle of 45. The sidewall compression angle varies between 7.7 and 10.2 degrees. The intake uses a straight lip. The throat has a height of 34.3 mm and is located 644 mm downstream of the ramp leading edge. Subsequent to the throat, the intake opens by 2 degrees to compensate for the growing boundary layer. At $x=166$ mm, there is a step on the upper and lower intake wall of 1 mm each. Here, the diamond shaped injectors will be mounted (also shown in Fig. 1). However, for the current performance analysis of the intake at a flight Mach number of 8 the geometry of the injectors was not considered.

The performance of the inlet can be assessed in form of aerodynamic parameters. Typical performance parameters are the mass flow ratio MFR , the total pressure recovery factor π_C and the kinetic energy efficiency η_{KE} . The mass flow ratio specifies how much of the maximum possible amount of flow at freestream conditions through the inlet is being captured. When isentropic expansion is assumed, the kinetic energy efficiency is the ratio of kinetic energy of the de-

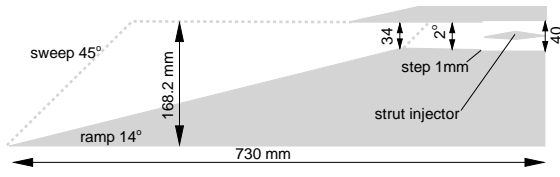


Fig. 1 Intake geometry

celerated flow to the kinetic energy of the undisturbed flow. For an ideal gas, η_{KE} is a function of the total pressure recovery coefficient $\pi_C = p_{t,3}/p_{t,0}$ and the freestream Mach number [17].

2 Numerical Method

2.1 Navier–Stokes Solver FLOWer

The DLR FLOWer code [10] is applied, which solves the unsteady compressible Navier–Stokes equations using a cell–centered finite volume method on block–structured grids. An advection upstream splitting method (AUSM) Flux Vector splitting is used for the inviscid fluxes and second order accuracy in space is achieved by means of a monotonic upstream scheme for conservation laws (MUSCL) extrapolation with a van Leer limiter function. The diffusive fluxes are discretized by central differences. Time integration is performed by a five–step Runge–Kutta method. For wall dominated flows with thick boundary–layers, strong shock / boundary–layer interaction and with separation, as they are of interest here, the assumption of a linear dependence between the Reynolds stress tensor and the strain rate tensor is not always valid. Therefore, a relatively newly implemented differential Reynolds stress models (RSM) [4, 3] is used in the simulations. This model solves transport equations for each component of the Reynolds stress tensor as well as for an additional length scale. Thus, it is computationally expensive. Furthermore, it decrease the stability of the numerical scheme. However, RSM computations show promising results, especially for separated flows [12]. The model uses

a simplified version of the Launder-Reece-Rodi (LRR) model by Wilcox close to the wall, the Speziale-Sarkar-Gatski (SSG) in the farfield and Menter’s ω -equation for closure. Accordingly, that model is called SSG/LRR- ω model. Like the flow equations, the spatial discretization of the turbulent transport equations is performed using an AUSM upwind scheme with van Leer limiter for the convective and central discretization for the diffusive terms. To increase the numerical stability of turbulent flow simulations, the time integration of the turbulence equations is decoupled from the mean flow equations, and the turbulence equations are solved implicitly. The FLOWer computations are performed on a NEC SX–8 cluster using 16 processors, taking approximately 5000 CPU hours to converge.

2.2 Boundary Conditions

At the inflow boundary, the freestream conditions of the experimental investigation listed in Table 1 are prescribed. These test conditions have slightly changed from the conditions specified for the previous analysis [13] to obtain values closer to the intended flight conditions (condition F). Condition II was chosen to yield temperatures comparable to the conditions in the connected pipe facility. The turbulent values are determined by the specified freestream turbulence intensity Tu_∞ : $k_\infty = 1.5(Tu_\infty u_\infty)^2$. The Reynolds stress matrix is initialized by placing $2/3 k_\infty$ on the diagonal and the specific dissipation rate of the freestream is $\omega_\infty = k_\infty / (RLTU \cdot \mu_{lam})$ with RLTU being a measure for the ratio of turbulent to laminar viscosity in the freestream (here: RLTU=0.001). For the supersonic outflow, the

Table 1 Test conditions

	M_∞	Re_∞/m	p_0 [MPa]	T_0 [K]	T_∞ [K]
F	8.0	$2.94 \cdot 10^6$	11.4	3130	227
I	8.0	$3.2 \cdot 10^6$	11	2850	206
II	8.0	$8.4 \cdot 10^6$	11	1550	105

variables are extrapolated from the interior. At

solid walls, the no-slip condition is enforced by setting the velocity components and the normal pressure gradient to zero. Due to the short measurement times in a high-enthalpy facility it is assumed the model remains at a constant ambient temperature of $T_{wall} = 293K$. Additionally, the Reynolds stresses are set to zero at the wall and the respective length scale is prescribed based on the first grid spacing according to Menter.

2.3 Numerical Accuracy

A complete validation of the FLOWer code has been performed by the DLR prior to its release [1, 11] and continued validation is achieved by the analyses documented in subsequent publications [15, 16, 2]. Furthermore, FLOWer has already been successfully used in the analysis of 3D hypersonic intake flows [12, 14, 8, 9].

3 Results

The design of the tested scramjet demonstrator is centered around the supersonic combustion process employing a central strut injector with hydrogen injection [5, 7]. The primary purpose of the intake is to provide high-pressure flow to the engine with a minimum of aerodynamic losses and a static temperature high enough to allow for stable combustion. Additionally, the combustion process itself causes a variation of the inlet back pressure which needs to be considered when analyzing the performance of the whole system. However, earlier analyses of the combustion chamber have shown the back pressure to be negligible due to the lean mixture of fuel and air currently used. Another critical factor is the static temperature at the end of the compression process which has to be high enough to ensure self ignition of the hydrogen. Thus, the current analysis focused mainly on the combustor inflow as well as yields some clues concerning placement of pressure transducers in the intake model.

For the numerical analysis of the half model approximately 3.5 Mio grid cells are used, 433 nodes in the main flow direction and 81 x 114 and 81 x 145 for the cross section before and after the

step, respectively. The decomposition of the grid is 16 blocks needed for the MPI parallelization. The grid spacing stretches away from the walls and is clustered at the leading edges of ramp and cowl. Otherwise, great care is taken to obtain a overall homogenous grid spacing (see Fig. 2). Earlier analysis showed a certain grid sensitivity of hypersonic shock wave boundary layer interaction when local grid refinement is applied [14]. A minimum wall spacing of $\Delta = 1.e-06$ is used in all directions yielding a y^+ of 1.

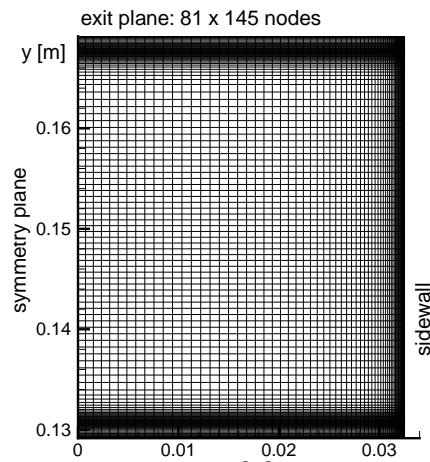


Fig. 2 Grid cell distribution at exit plane.

External compression of the inlet is ensured by a ramp angle of 14° and two side wedges with deflection angles of $7.7 - 10.2^\circ$ and a sweep angle of 45° each. The overall dimensions of the intake can be see in Fig. 1. In Fig. 3, the Mach number isolines of the center plane show the gap between ramp shock and engine cowl to be too large, resulting in an unnecessarily high spillage drag. Approximately, one third of the captured mass flow is lost here. The reason for the gap is the displacement of the ramp shock (which was designed using the shock-to-lip condition) by the side wall compression. At first, it was assumed that the lip shock impinging on the thick hypersonic ramp boundary layer might have a strong upstream effect. This was supported by the distribution of wall pressure shown in Fig. 4. However, by using a bleed boundary condition at the impingement point of the lip shock ($\Delta x_{bleed} = 20$

mm between 0.562 and 0.582 mm downstream of the leading edge) the separation was strongly reduced (see Fig. 5) without reducing spillage drag. Currently, simulations are performed where the ramp is 30 mm shorter (everything else is kept constant) to bring the ramp shock closer to the engine cowl. The distribution at

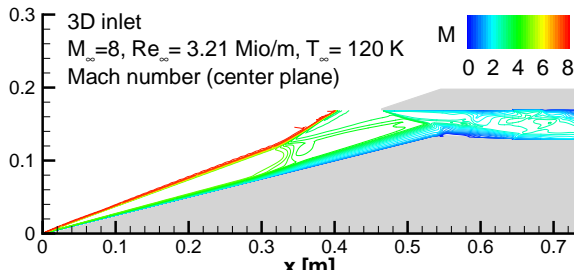


Fig. 3 Mach isolines at center plane for 3D intake.

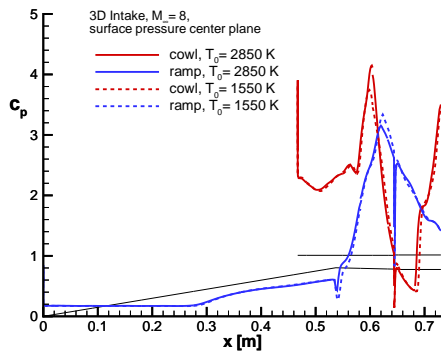


Fig. 4 Surface pressure distribution along center.

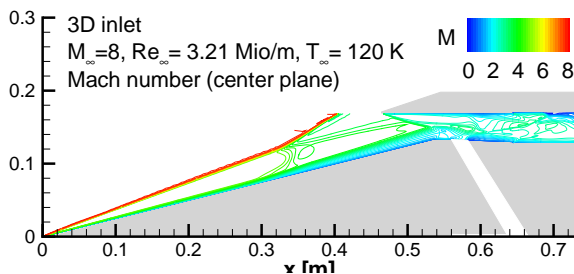


Fig. 5 Mach number contours at center plane with bleed.

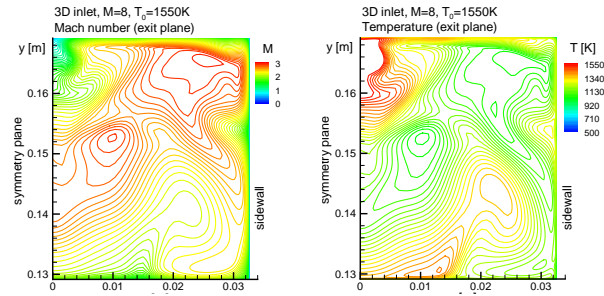


Fig. 6 Mach number and temperature isolines on exit plane of 3D intake (condition II).

the exit plane of the intake shows a strongly inhomogenous behavior. Within those corner vortices, the average Mach number is approximately 2 whereas for the remaining part of the exit cross section a Mach number of 3 to 4 is retained. The isolines shown in Fig. 6 have been computed for the condition II of Table 1, however, also the two test conditons, I and flight, yield comparable distributions. Due to the strong vortex system, hot spots are created in the exit flow with maximum temperatures of 1200 K, even though the average temperature is only 709 K for the cold test condition II (see Table 2). The strut injector is mounted across the z-direction at the center height of the chamber, therefore hydrogen will be injected within the vortex region, thus, initiating the combustion process even for the low temperature test case. The performance of

Table 2 Average values at exit plane

	\bar{M}_{exit}	\bar{T}_{exit} [K]
I	2.35	1223
II	2.42	709

Table 3 Performance parameter

	MFR	π_C	η_{KE}
I	0.68	0.11	0.615
II	0.68	0.12	0.616

the intake, specified in Table 3 is not satisfying

from the inlet designer point of view. However, the exit condition should suffice to achieve a stable supersonic combustion which is the main goal of the pending test campaign. Nevertheless, the computational intake analysis is continued to obtain an improved inlet design without changing too many design parameters and jeopardizing the the combustion process.

4 Conclusions

In this paper the performance analysis of the intake at a flight Mach number of 8 is performed. The role of the present numerical computations is to complement the experimental investigations and to enhance the understanding of the obtained results. Additionally, the numerical simulation completes the knowledge of the flow field in areas which are not accessible to measurements and allows for an overall performance analysis of the inlet geometry. The current analysis denotes the developing corner vortices as a key feature to ensure self ignition for the low temperature ($T_0 = 1550$ K) experimental test run.

Acknowledgments

This work has been financially supported by the Deutsche Forschungsgemeinschaft (DFG) within the frame of the German Research Training Group GRK 1095/1.

4.1 Copyright Statement

The authors confirm that they, and/or their company or institution, hold copyright on all of the original material included in their paper. They also confirm they have obtained permission, from the copyright holder of any third party material included in their paper, to publish it as part of their paper. The authors grant full permission for the publication and distribution of their paper as part of the ICAS2008 proceedings or as individual off-prints from the proceedings.

References

[1] Becker N, Kroll N, Rossow C. C., and Thiele F. Numerical flow calculations for complete

aircraft - the megafLOW project. *Proc DGLR Jahrbuch 1998*, Vol. 1, pp 355–364, Bonn, Germany, 1998. Deutsche Gesellschaft für Luft- und Raumfahrt (DGLR).

- [2] Coratekin T. A, van Keuk J, and Ballmann J. On the performance of upwind schemes and turbulence models in hypersonic flows. *AIAA Journal*, Vol. 42, No 5, pp 945–957, May 2004.
- [3] Eisfeld B. Implementation of reynolds stress models into the dlr-flower code. IB 124-2004/31, DLR, Institute of Aerodynamics and Flow Technology, 2004.
- [4] Eisfeld B and Brodersen O. Advanced turbulence modelling and stress analysis for the dlr-f6 configuration. AIAA Paper 2005-4727, 2005.
- [5] Gerlinger P, Kasal P, Stoll P, and d. Brüggemann. Experimental and theoretical investigation on 2d and 3d parallel hydrogen/air mixing in a supersonic flow. International Society for Air Breathing Engines, Paper ISABE-01-0189, 2001.
- [6] Goonko Y. P, Kharitonov A. M, Mazhul I. I, Zvegintsev V. I, Nalivaichenko D. G, and Chirkashenko V. F. Investigations of a scramjet model at hypersonic velocities and high reynolds numbers. AIAA Paper 2002-5273, 2002.
- [7] Kasal P, Gerlinger P, Walther R, von Wolfersdorf J, and Weigand B. Supersonic combustion: Fundamental investigation of aerothermodynamic key problems. AIAA Paper 2002-5119, 2002.
- [8] Krause M and Ballmann J. Numerical simulations and design of a scramjet intake using two different rans solver. AIAA Paper 2007–5423, 2007.
- [9] Krause M, Reinartz B, and Ballmann J. Numerical computations for designing a scramjet intake. *Proc 25th Congress of International Council of the Aeronautical Sciences (ICAS), Hamburg, Germany, 3-8 September 2006*, 2006.
- [10] Kroll N, Rossow C.-C, Becker K, and Thiele F. The megafLOW project. *Aerospace Science and Technology*, Vol. 4, No 4, pp 223–237, 2000.
- [11] Radespiel R, Rossow C, and Swanson R. Efficient cell-vertex multigrid scheme for the three-dimensional navier-stokes equations. *AIAA Journal*, Vol. 28, No 8, pp 1464–1472, 1990.

- [12] Reinartz B and Ballmann J. Computation of hypersonic double wedge shock / boundary layer interaction. *Proc 26th International Symposium on Shock Waves (ISSW 26), Göttingen, Germany 16-20 July 2007*, 2007.
- [13] Reinartz B, Ballmann J, and Behr M. Computational analysis of a 3d hypersonic intake for experimental testing at mach 8. Aiaa paper.
- [14] Reinartz B, Ballmann J, Brown L, Fischer C, and Boyce R. Shock wave / boundary layer interaction in hypersonic intake flows. *Proc 2nd European Conference on Aero-Space Sciences (EUCASS), Brussels, Belgium 1-6 July 2007*, 2007.
- [15] Reinartz B. U, Ballmann J, Herrmann C, and Koschel W. Aerodynamic performance analysis of a hypersonic inlet isolator using computation and experiment. *AIAA Journal of Propulsion and Power*, Vol. 19, No 5, pp 868–875, 2003.
- [16] van Keuk J, Ballmann J, Sanderson S. R, and Hornung H. G. Numerical simulation of experiments on shock wave interactions in hypervelocity flows with chemical reactions. AIAA Paper 03–0960, January 2003.
- [17] Van Wie D. M. Scramjet inlets. In Curran E. T and Murthy S. N. B, editors, *Scramjet Propulsion*, Vol. 189, pp 447–511, Reston, VA, 2000. AIAA.